

An Adaptive Locally Connected Neuron Model: Focusing Neuron

F. Boray Tek

Department of Computer Engineering, Isik University, Sile, Istanbul, Turkey, 34980

Abstract

We present a new artificial neuron model capable of learning (train) its receptive field in the spatial domain of inputs. In a feed-forward neural network, a layer of focusing neurons can generate unique connection maps for a problem. The new model uses no other tool than the back-propagation algorithm to learn its focus parameters which control the receptive field locations and apertures. We formed focusing neuron networks of one or two hidden layers and tested them on synthetic and well-known image recognition datasets. In the synthetic datasets, we observed that the focusing neurons moved their apertures towards the informative inputs and avoided the intentionally-placed random features. Tests on common datasets, such as MNIST, have shown that a network of two hidden focusing layers can perform significantly better (for MNIST: 99.21% test accuracy) than a fully connected dense network with the same configuration. Furthermore, the experiments demonstrate that using focusing layers instead of dense layers in convolutional architectures can improve the classification performance in challenging data sets.

Keywords: locally connected neuron, artificial neuron model, adaptive neuron, attention, receptive field size, focusing neuron

¹Email: boray.tek@isikun.edu.tr

1. Introduction

The structure of the brain is mutable. Neuroplasticity, the ability of neurons to reorganize and adapt to inner or outer environments, causes the brain to change through its lifetime [1, 2]. The changes can occur in larger (e.g., cortical remapping) or in microscopic synaptic scales in which individual cells alter their connections through activity and learning [2, 3]. The changes allow divisions and specializations to make the biological brain capable of solving thousands of sensory, cognitive, and behavioral problems within the same framework [4].

Recent developments in the design and training of artificial neural networks (ANN) enabled us to solve many pattern recognition problems with acceptable accuracies. However, artificial networks are not yet comparable to the self-organizing and multi-functional biological brain. Many biology-inspired artificial models are unfit for large-scale pattern recognition tasks [5]. Hence, still, many recent works propose sophisticated artificial network structures optimized for solving single-target tasks [6, 7, 8, 9, 10, 11]. Although some architectures can deal with multi-modal information [10, 12], the typical design approach is to create a fixed topology (network connection map) to solve a task. The connection map is pre-determined by an expert, who uses heuristics or prior knowledge of the domain. Some hard-wired networks are composed of several interacting sub-networks [7], the fixed network structures still lack the self-organizing capacity of the brain.

Mimicking the self-organizing brain may be possible with an automated algorithm which can construct a network iteratively or with evolutionary mechanisms [13, 14]. Still, we require new models which can self-create a topological structure. Though literature contains examples of architecture optimizers [15, 16, 17, 18], network growing/pruning algorithms [19, 20, 21, 22], and evolutionary processes [14], the approach of the current paper is based on a new

artificial neuron type that can learn its receptive field and so its local connections in a topological structure. The new model, which we named a “focusing neuron”, brings an adaptive-wiring ability to artificial neurons.

Some studies on local learning or local receptive fields [23, 24, 25] interpret the locality of a neuron as its selectivity in the input value domain. For in an input space formed of two input features (x, y) , such a neuron learns to be active for only a subset of the input values (e.g., $[x_a < x < x_b, y_c < y < y_d]$). Hence, this localization corresponds to a partitioning (clustering) of the input (value) space but requires the neuron to be globally connected to observe the whole space. Instead, the locality of the proposed model is based on the input topology.

A focusing neuron has a focus attachment to change its local receptive field in the topological domain of inputs. It can learn and create unique connection maps for inputs and problems presented by data. Akin to the synaptic plasticity guided by biochemical cues between axons and dendritic spines [26, 27], the new model uses error gradients to guide the receptive field. To that end, the proposed framework assumes a spatial continuous positional space for the inputs in which the focus function is differentiable. Thus, focusing neurons are fully trainable by the gradient descent algorithm with no additional heuristics.

In this paper, we introduce a topology aware, and locally adaptive -focusing-neuron model. We do not claim the state-of-the-art in a particular pattern recognition application, nor do we suggest replacing the fully connected neuron model or convolutional networks. However, the new model and its components (positional inputs and the training of the locality) can guide us in reducing structural heuristics and redundancy in neural networks.

This paper presents the insights gained since our initial presentation of the new model [28]. The main contributions made by this paper are as follows:

1. It formally describes the focusing neuron model.
2. It derives a scheme for the initialization of weights and focus parameters.
3. It shows that focusing neuron instances can seek informative features and avoid redundant inputs.
4. It compares the networks of focusing layers with the networks of fully connected layers with tests on popular MNIST, MNIST-cluttered, Fashion, CIFAR-10, Reuters-21578, and Boston Housing datasets [29].
5. It demonstrates that, owing to their (trained) narrower receptive fields, connections constructed by a focusing neuron layer can be 70% sparser than its dense counterpart which performs worse.
6. It shows that when used in convolutional networks the focusing layers can improve the classification performance in challenging data sets.

2. Background

We start by discussing the concept of locality and examine the fully and locally connected models from the corresponding perspective. Then we describe the focusing neuron model.

2.1. Local Learning

Hubel and Wiesel [30] discovered that the *simple cells* in the primary visual cortex are selective for the position, scale, orientation, and polarity of inputs. Differently, the *complex cells* that process signals from the simple cells can be selective as far as to activate only in the presence of a particular face or object [31]. The selectivity (or locality) of a biological neuron relies on the different cell types, local wiring (selective pooling), and the hierarchical structure of the neural circuitry [32].

A psychologist, Donald Hebbian [33] was the first to refer to a metabolic mechanism that strengthens the connection between two neurons: “When an

axon of cell A is near enough to excite cell B and repeatedly or persistently takes part in firing it, some growth process or metabolic change takes place in one or both cells such that A’s efficiency, as one of the cells firing B, is increased”. The description is slightly vague. However, note that the axon of A (not A itself) is required to be *near* enough to strengthen the connection with neuron B.

On the artificial side, a theoretical framework by Baldi and Sadowski [34] describes that local learning requires 1) that learning depends on local information (of pre- and post-synaptic neurons), and 2) the functional form which operates the learning rule use only the local information due to the activations of these neurons. Thus, for a generic update rule of the form, $\Delta w = f(x, \Theta)$ the input signal x and update parameters Θ must be local.

2.1.1. Local Receptive Fields

The studies of artificial neuron and local receptive fields go back to Rosenblatt’s perceptron [35], which was the first *weighted* neuron model devised for feed-forward networks. Some variations of perceptron were designed to be locally connected, i.e., had a limited *fan-in* in the input surface [36]. The perceptron also included random (stochastic), partially connected neurons. As Minsky [36] had also noticed, non-overlapping local receptive fields put a limitation on the (spatial) scale of information that can be extracted from the input. Fukushima [37] tackled this problem with a hierarchical network structure (aka neocognitron), which later inspired convolutional neural networks [38].

2.2. Fully Connected Neuron

The conventional fully connected neuron model [39, 40] is often used in feedforward neural networks. The neuron multiplies the inputs $(x_1, x_2, \dots x_m)$ with the connection weights $(w_1, w_2, \dots w_m)$ and then sums the weighted inputs,

adding a bias term (b) to calculate a net/total input. It then passes the net input (net) through a non-linear transfer function (f) to produce the output (a) of the neuron (1).

$$a = f \left(\sum_{i=1}^m w_i x_i + b \right) \quad (1)$$

The receptive (or input) field covers every input or neuron in the backward connected layer and is thus defined as “fully connected”. A layer formed of such neurons is commonly referred to as a “dense layer”. For a fully connected neuron of m inputs, there can be 2^m permutations (of the input) which are all the same because the positioning (ordering) of the inputs (here the index i) is unimportant. The free parameters of the model are the weight values (and the bias) which are updated (trained) using the delta rule (3):

$$\hat{w}_i = w_i - \eta \frac{\partial E}{\partial w_i} = w_i - \eta \frac{\partial E}{\partial a} \frac{\partial a}{\partial net} \frac{\partial net}{\partial w_i} \quad (2)$$

$$\hat{w}_i = w_i - \eta \frac{\partial E}{\partial a} f'(net) x_i \quad (3)$$

At first glance, a fully connected neuron should be able to zero-out some of its weights through updates and thence can become locally or at least partially connected. However, no matter how redundant the inputs or connections, the training cannot cancel any connection, partly due to the learning rule and the ordinary cost functions (e.g., minimum squared error, cross-entropy).

To understand this phenomenon, let us examine the delta rule for a neuron with two inputs and two connections. Assume that one connection (w_1) is attached to a constant, non-informative, and non-zero input ($x_1 = c$), where the other connection is attached to an informative and changing input (x_2). Since x_1 is constant, let us set the corresponding weight to zero, i.e., $w_1 = 0$, which results in a broken connection. In the first (next) update, w_1 cannot remain zero

unless either the error term $\frac{\partial E}{\partial a}$ or the derivative term $f'(net)$ is zero ($\eta > 0$).

Both terms are shared in the update of both weights (w_1, w_2). Hence, the error term cannot be zero unless the training is completed. The derivative term depends on the activation function (f) in the form of sigmoid, tanh, or relu, which have positive (or zero) derivative values. A zero derivative value can keep the weight w_1 at zero, yet this prevents the update of w_2 as well. Even if the weight value reaches zero via an update, it will change in the next one unless the error term had also reached zero in the same iteration. The induction is similar for a neuron with more inputs or a truly random (non-informative) redundant input.

The problem of redundancy in a network in terms of the number of neurons and connections (e.g., pruning) was popular in early studies [41, 20, 42]. Perhaps increased computational power or excitement around new deeper architectures may have temporarily overshadowed the problem. However, it has recently regained momentum with the development of resource-critical applications [18, 43, 44, 45, 46].

It is possible to reduce network redundancy through the simple strategy of adding a regularization factor to the loss calculation. Typical examples are the L1 or L2 norms of weights in a network or layer [47]. Such a regularization term creates a penalty for the weight magnitudes, pushing them toward zero. More zero-valued weights would make a network sparser and less redundant. However, the penalty applies to all connection weights in a layer (or whole network); it does not explicitly target redundant connections. Therefore, adding a regularization penalty to a cost function requires attention because it may compete with the target loss of a network.

2.2.1. Locally Connected Neuron Model

A locally and partially connected model may refer to different structures [48, 49, 42]. *Local* implies a connected and bounded group (subset) of connections, whereas partial may refer to any subset of all input connections [42]. For example, connecting a random subset of neurons will create a partially connected structure. Therefore, partial includes local, but not vice versa.

The fully connected model (1) can express a partially connected neuron by setting some weights at zero. However, it neither generates nor maintains a partially connected structure during the training due to the gradient updates deriving from the back propagation learning rule. Therefore, to create locally (and partially) connected structures in practice, some designers have used domain knowledge or assumptions to partition the input space and create manual wirings for specific problems [50, 51, 52, 53]. The fixed local connection maps (or layers) constrain the neurons to receive signals from a fixed subset of inputs, i.e., a region in the input domain. In contrast, the proposed model allows a neuron to learn its local connections by trainable parameters.

2.2.2. Convolutional Layers

The neurons used in convolutional layers are (fixed) locally connected neurons which share their weights with all the neurons in the same layer. The weight sharing reduces the number of free parameters drastically and allows learning of efficient representations, that are equivariant to input translations [38, 52, 54]. Convolutional neuron layers provide effective feature extraction in spatially ordered input domains such as image and speech analysis.

There were attempts to create adaptive local connections for convolutional neurons. In locally smoothed neural networks [55] convolutional filter weights were factorized into smoothing and kernel parts. The smoother part was modeled by a 2-D Gaussian function. The parameters of the Gaussian smoothers

were dynamically generated by a regression network. The Gaussian smoothing of the input space can be seen as a special case of (dynamic) focusing neurons for two-dimensional input spaces. In [56], a Gaussian envelope was used to guide convolution kernels to create an adaptive receptive field size and orientation.

2.2.3. *Clustering based locality*

Some studies implement the locality of a neuron as its selectivity (specialization) in the input value domain [23, 24, 25, 57]. The selectivity is built by partitioning/clustering the input (feature) density space. A well-known example of clustering-based approaches is the radial basis function (RBF) network [57]. In an RBF network, each neuron localizes itself in the input value domain using the center and spread of Gaussian kernels. RBF neurons cluster or partition the input value domain instead of the inputs' spatial domain. Likewise, learning in vector quantization networks involve competition between individual neurons to gain control of a cluster in the input domain [58]. RBFs (and LVQ neurons) are invariant to input topology. An RBF neuron must receive input from all inputs to localize itself in the input value domain.

A self-organizing map (SOM) projects the input feature space to a two-dimensional lattice [59]. Hence, SOM neurons can be described as neurons with spatial dimensions; however, they also ignore the spatial dimension of inputs.

In a hierarchical network structure, the neurons get activated selectively for different inputs. For example, in the primate brain, one can find individual neurons activating for particular faces [31]. The hierarchy naturally induces a specialization (localization) in the input space. Some works aim at manipulating or guiding this selectivity (and specialization) to create orthogonal and sparser receptive fields and thence representations [23, 24, 25].

2.2.4. Adaptive locality in the topological space

This section describes how locality involves local connections/wiring of the neurons, as in our model. The biological name for adaptive local connectivity is plasticity (neuroplasticity). While relatively less-explored in the artificial domain, plasticity has been an active problem in neurobiology for a long time [60], as well as in spiking artificial neuron models [61, 62, 63]. Still, some studies directly aimed to reproduce Hebb’s rule or other plasticity models for their artificial counterparts [64, 65, 66]. For instance, Miconi’s [65] neuron model is shown below with our notation. The total effective weight is the sum of the fixed weight w_{ij} (as in a fully connected neuron) and a plasticity coefficient $\alpha_{i,j}$ and a recursively calculated Hebbian trace (Hebb_{ij}):

$$a_j(t) = f \left(\sum_{i=\text{inputs}} [w_{ij}x_{ij} + \alpha_{i,j}\text{Hebb}_{ij}(t)a_i(t-1)] \right) \quad (4)$$

Thus, the model requires a recurrent calculation of Hebbian $\text{Hebb}_{ij}(t)$ trace using Oja’s rule [64]; however, the non-plastic weight component must be set at zero $w_{ij} = 0$ to be fully plastic.

The locality has been frequently investigated in the context of visual attention models where the objective is to interpret or exploit the information in various locations of an input image [67, 68]. Recently proposed deep neural network architectures of visual attention models [11, 10] have shown impressive results in multiple object recognition, image captioning and similar tasks. The common strategy in these models is to process an input image in n steps where, at each step, the recurrent layer examines the current input and then decides on the next location to process.

Cheung et al. [69] proposed a retinal glimpse model (for visual attention) which employs Gaussian kernels to control sampling locations and scales. Sim-

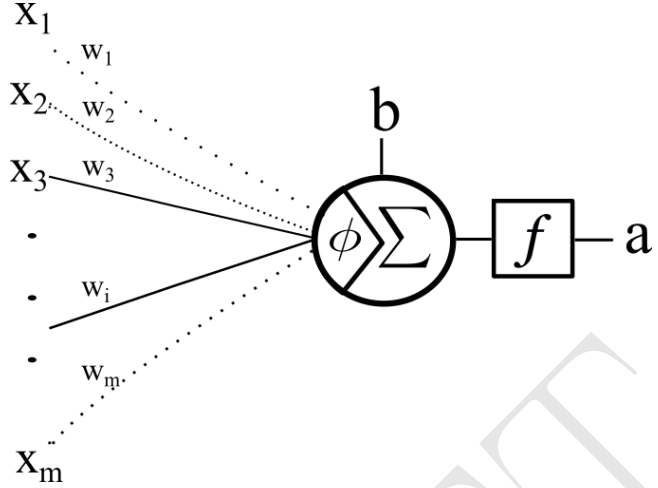


Figure 1: The focusing neuron model. The focus attachment ϕ allows the neuron to change its receptive field and adjust the aperture size. It generates coefficients which are multiplied by inputs and connection weights to collect the net input. The sum of net input and bias b is mapped to the output by the activation transfer function f .

ilarly, the focusing neuron model employs Gaussian kernels to control and learn the location and scale of the local receptive field. Our model is generic; hence it may be used for any task, and is not limited to visual attention.

The capsule architecture proposed by Sabour et al. [54] performs dynamic routing which is an example of adaptive locality. A capsule is a group of neurons with a routing function that selectively and jointly directs the output vector of the group to only one of the several groups in the forward layer. The routing function is iteratively calculated per input. Our model is static (learned during training) however it can be made dynamic (calculated per input). Interestingly, the focusing neuron model can be made forward-faced. Thus, it can adaptively focus the output transmitting field for the next layer. However, the backward focusing model is more compatible with the backpropagation algorithm and more efficient to run on the current graph frameworks such as Theano [70] or Tensorflow [71].

3. Method

3.1. Focusing neuron

A focusing neuron is an adaptive locally connected neuron. Figure 1 depicts the new model as a neuron with a backward focus attachment. The role of the focus is to enhance/suppress the connection weights for some inputs in the domain and to collect/filter data from the rest. The name is motivated by the fact that the neuron can change both its local receptive field location and its size (aperture). The new model assumes a topological (positional) continuous input space where the focus function is differentiable.

We describe a focus mechanism for a one-dimensional input topology. Generalization to higher dimensions is straightforward. Let $\tau(i) \in \mathfrak{R}$ denote a mapping for the position of the input indexed with i . The focusing model has the following functional form:

$$a = f \left(\sum_{i=1}^m w_i \phi(\tau(i), \Theta) x_i + b \right) \quad (5)$$

The deterministic focus function ϕ with its parameter set as Θ generates a focus coefficient for each input i at position $\tau(i)$. This may resemble the addition of a second weight for the connection. However, the coefficient values are dependent and controlled by the parameter set as Θ for each neuron. With the appropriate functional form and parameters, the neuron can change its input subset by moving, growing or shrinking its receptive aperture. The model complies with the popular tensor processing libraries which perform layer-wise operations. For a layer of focusing neurons, a simple element-wise multiplication of the focus coefficient matrix Φ can mask and scale the connection weight matrix W .

3.1.1. Focus control function

A Gaussian form is the first candidate for the focus control function because it is continuous and differentiable, and it neither creates nor enhances extrema [72]. Some of these properties also exist in discrete space if the sample size is sufficiently large. In the case of the current paper and for simplicity, we can assume $\tau(i) = i/m$, so that the input position is taken as its normalized index over m neurons in the input layer. In a multi-dimensional topology, both the control function and position are multivalued, e.g., $\tau(i, j) = (i/m, j/n)$. In a single dimensional space, a Gaussian focus, $\phi(i, \Theta)$ can be defined in the following way:

$$\phi(i, \mu, \sigma) = s e^{-\frac{(i/m - \mu)^2}{2\sigma^2}} \quad (6)$$

where μ represents the focus center and σ acts as the aperture size control (6). The form includes the scalar (s) to equalize the norm of ϕ to the norm of the fully connected model. When σ is very large, the scalar converges to one ($s \approx 1$), which transforms the neuron into a fully connected neuron of m inputs. However, when σ is not large, the exponential term produces coefficients that are less than one. Thus, the scalar s ensures a (fully connected) norm of (\sqrt{m}) with respect to the neuron's receptive field.

$$s^j = \frac{\sqrt{m}}{\sqrt{\sum_{i=1}^m \left(e^{-\frac{(i/m - \mu_j)^2}{2\sigma_j^2}} \right)^2}} \quad (7)$$

Note that the Gaussian is nearly non-zero over the input positional domain. This is desirable since the neuron must receive inputs and corresponding gradient cues (however small) from the positions that are farther from the focus center. However, at run-time, the out-of-focus coefficients can be neglected (or pruned) if desired, which is different from pruning the small weights of a trained

network. Since the product of the trained focus coefficients and weights form the effective weights, the focus function is not necessary at run-time, unless online learning is in progress.

The partial derivatives of the Gaussian focus function for μ and σ are well defined (8). Hence they can be incorporated into the chain rule easily (9) and can be trained with the back-propagation learning rule and generalized cost functions.

$$\frac{\partial \phi}{\partial \mu} = \frac{(i/m - \mu)}{\sigma^2} \phi, \quad \frac{\partial \phi}{\partial \sigma} = \frac{(i/m - \mu)^2}{\sigma^3} \phi \quad (8)$$

$$\hat{\mu} = \mu - \eta \frac{\partial E}{\partial a} \frac{\partial a}{\partial f} \frac{\partial f}{\partial \phi} \frac{\partial \phi}{\partial \mu}, \quad \hat{\sigma} = \sigma - \eta \frac{\partial E}{\partial a} \frac{\partial a}{\partial f} \frac{\partial f}{\partial \phi} \frac{\partial \phi}{\partial \sigma} \quad (9)$$

3.1.2. Initialization of parameters

Recent studies have shown that the initialization of weights in a neural network is crucial for improving its training and generalization capacity [73, 74]. The weights of a focusing neuron should not be initialized using He or Glorot methods directly, because the focus coefficients scale the weights and change the variance of the propagated signals (see Appendix A). Moreover, since the total fan in (or the number of inputs) of a focusing neuron is usually larger than its effective fan in, we introduced the scaler (7) to ensure the total norm to be equivalent to the norm of a fully connected neuron. However, in general, the weights of an individual focusing neuron (j) can be sampled with respect to the squared norm of its focus coefficients vector:

$$w^0 \sim U \left[-\frac{\sqrt{6}}{\sqrt{\sum_{i=1}^m \phi^2(i)}}, \frac{\sqrt{6}}{\sqrt{\sum_{i=1}^m \phi^2(i)}} \right] \quad (10)$$

To initialize the receptive fields, we must also initialize μ_j and σ_j for the Gaussian control function $\phi(i/m, (\mu_j, \sigma_j))$. The centers of the foci μ_j can be spread or randomly initialized in the range $[0, 1]$, while the aperture controls

must be set to positive non-zero values, $\sigma_j > \epsilon$. Distributing the foci centers works more effectively than initializing them all in the center. Initializing σ to a value in the range ($[0.05, 0.2]$) enables the neuron to sniff inputs from a range. A smaller σ value generates overly narrow apertures which may cause neurons to be stuck in their initial position. A larger σ generates a wider aperture which may cause the neurons to be indifferent and fully connected. In fact, the ideal μ and σ initializations depend on the intended role of the neuron. In addition, one can apply L1 or L2 regularization on σ to control or encourage locality, if the $\sigma=0$ case is handled explicitly.

4. Experiments

Our experiments address fundamental questions about the new model. First, can focusing neurons create connection maps when they learn to focus their receptive fields? For instance, can they navigate towards more informative inputs or steer their focus away from redundant inputs? Second, how does a network of focusing neurons perform in common pattern recognition tasks? To understand whether the new focusing skill adds value, we compared networks of focusing neuron layers with networks of dense layers. We share the code of the focusing neuron and experiments online [75].

4.1. Learning to Focus

First, we constructed a synthetic (Gaussian blob) classification data set of two classes and 20 dimensions. Then we sampled 20 more Gaussian random input columns of normal distribution $N(0, 1.0)$ and added to the left side or both sides of the data to form two separate data sets of 40-dimensions. Then, each data column was normalized for zero-mean and unit variance.

We constructed a single hidden layer network of neurons with four hidden focusing neurons (2 outputs), rectified linear activations, and batch normaliza-

tion. For the focusing layer, all σ s were initialized to 0.08. For the left-noised case, we initialized μ s in the center with a small random margin; for the sides-noised data set, we spread μ s to cover the input space ([0.2–0.8]). The focusing neurons' weights w and μ used a learning rate of $\eta_{\mu,w} = 1e - 3$, whereas the apertures σ used a lower rate of $\eta_\sigma = \eta_\mu * 0.1$ to train the network with stochastic gradient descent with momentum (0.9) for 250 epochs with a batch size of 128. Figures 2a and 2b show the initial foci and learned foci after 250 epochs for the sides-noise and left-noise data sets respectively. In the former, since the informative features were in the center, the foci moved towards the center. In the latter, the features were on the right, the foci moved to the right.

We observed that in both cases most foci migrated towards informative inputs. Most of the neurons were enlarged, except the one that stayed relatively close to the center in the left noise case. The apertures were enlarged because only four focusing neurons were required to partition the whole input field. However, one must note that focus parameters affect the received signal magnitude. Figure 2c shows the change of the foci parameters (for the left-added noise) during the training epochs. We were able to observe a stable convergence of the two parameters.

In some cases, we observed that when all the neurons were initialized in the pure noise region (not shown), they could get stuck when the initial aperture was narrow. Therefore, this experiment has shown two interesting results: focusing neurons can seek and focus on informative inputs; however, they can also become jammed in noisy input regions with a narrow aperture. We observed similar results with larger synthetic input domains and with different settings. Figure 2d shows the initial and final focused weights ($\phi_i * w_i$) for each neuron (for the left noise-added dataset). The final non-zero weights are apparent on the right and cleaner half of the input space. In the following experiments, we

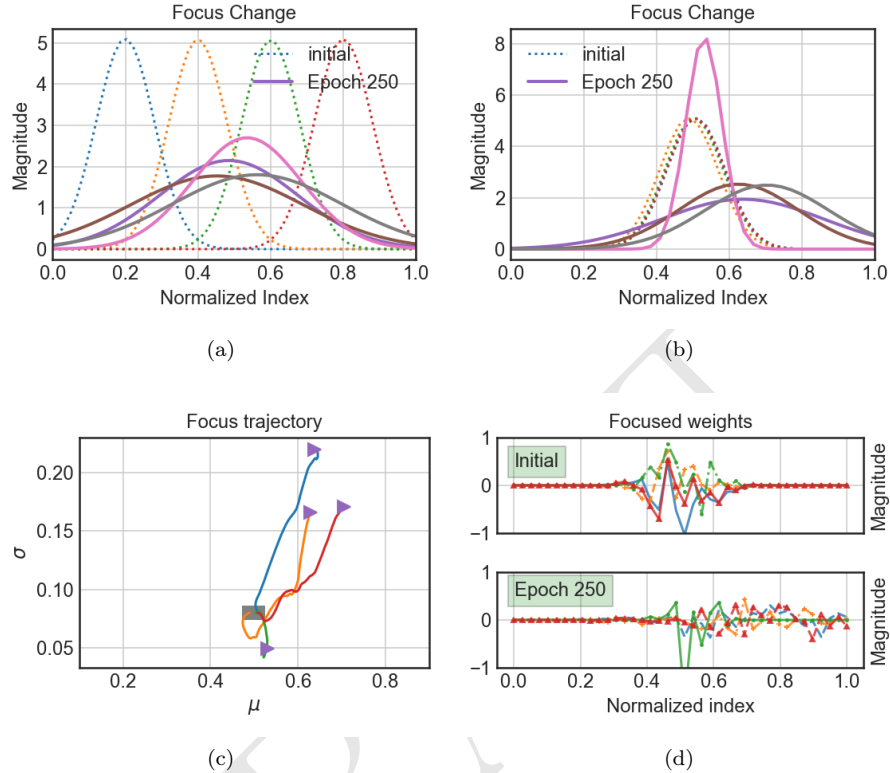


Figure 2: The initial and final foci (and weights) after training: a) Random noise on the sides, foci were initially spread, foci move to the center. b) Random noise on the left, foci initialized in the center, move to the right. c) The trajectory of foci parameters during training (square: start, >: end). d) Focused weights for b).

investigated whether the demonstrated adaptive skill yields any advantage over fully connected neurons.

4.2. Comparison with Fully Connected Neuron

4.2.1. Common Datasets

To test the focusing model in a real data scenario, we started with the popular gray-scale MNIST character recognition dataset [38] (MNIST). In addition, we performed experiments on more challenging datasets: MNIST-cluttered (CLT) which comprised randomly transformed MNIST samples superimposed

on cluttered 60x60 backgrounds [76]; the CIFAR-10 (CIFAR) general object classification dataset composed of 32x32x3 RGB images of various objects [77]; and a Fashion (FASHION) clothes dataset arranged similarly to MNIST [78]. These almost standard datasets were already separated into training (50000) and test instances (10000). We separated a validation set of 10000 randomly chosen instances from the training sets when a validation set was not available.

We then constructed a fully connected neural network of two hidden layers: Input - Hidden (800) - BatchNorm - DropOut(0.2) - Hidden (800)- BatchNorm - DropOut(0.25) - Output (10). In MNIST-cluttered, the number of hidden neurons was set to 1200 instead of 800, because the input images were considerably larger. For the comparison, the dense hidden layers were replaced by focused layers. We compared three different focusing network configurations: 1) A focused layer network (**Focus-s**) with foci initialized to spread ($\mu=[0.2, 0.8]$) over the input, 2) Foci initialized at the center (**Focus-c**), and 3) Foci initialized to spread ($\mu=[0.2, 0.8]$) but (parameters) are not updated during training epochs (**Fixed-s**). All σ s were initialized to 0.1. We applied value clipping for focus parameters after each update such that ($\mu=[0.0, 1.0]$) and $\sigma=[0.01, 0.5]$. We used the stochastic mini batch gradient descent with a batch size of 500.

We manually tuned the learning rate for each dataset to get the best performance from the dense network. Then, except for the learning rate, all focusing network hyper-parameters were tuned to get the best performance from the focused networks. For MNIST, CLT, CIFAR we set $\eta_g = 0.1$, $\eta_\mu = 0.01$, $\eta_\sigma = 0.001$ for the general (non-focus), focus center and aperture learning rates, respectively. For the Fashion data set we set $\eta_g = 0.1$, $\eta_\mu = 0.01$, $\eta_\sigma = 0.0005$.

All networks were trained for 350 epochs (focus parameters usually converged in less than 100 epochs). The training and test cycle was repeated five times. The average of the best test accuracy in five cycles and the maximum among

them (which was also the maximum of either early termination or the final epoch test, whichever was higher) are shown in Table 1. Other details can be found in the source code provided [75].

MNIST: All three focused networks performed slightly better than the dense network. Focus-s was the best performing, followed by Fixed-s then Focus-c. Figure 3 shows training and test errors that occurred during training iterations (of the best performed dense and Focus-s networks). The dense network reduced the training error rate better; however, the validation error rate increased gradually.

To inspect the locality of the connections, in Figure 4a we plotted some of the focused weights ($w_i * \phi_i$) of the first layer of the best Focused-s network after the training. The locality of the weights was clearly observable. However, some over-magnified weights hint overfitting.

CLT: Table 1 shows that all three configurations of the focused network performed 5-10% better than the dense network. Surprisingly, the best result was obtained by Fixed-s, which was slightly better than Focus-s. By checking the validation error rate in Figure 3b one can see that both the dense network and its focused counterpart overfitted, though this was more prominent in the former case.

CIFAR-10: All three configurations of the focused networks performed marginally better than the dense network. Focus-s network obtained the best accuracy. Again, the training and validation errors in Figure 3c indicate overfitting.

Fashion: The Focus-s network obtained the best accuracy. The dense network performed slightly better than the Fixed-s and Focus-c networks. As before, the dense network reduced the training error rate better; however, it started overfitting earlier than the focused network, as shown by the increased errors in the validation set (Figure 3d).

T-tests: Finally, we performed two-sample t-tests to test the significance of the difference in the mean test accuracies of the networks. The first row of Table 2 compares the Dense network and Focused-s networks. In the MNIST, MNIST-cluttered, and CIFAR-10 datasets the difference was statistically significant. The improvements in the challenging data sets were remarkable: MNIST-cluttered 8.64%, CIFAR-10 2.76%.

4.3. Sparsity

As mentioned earlier, the focus function is only necessary during training. At run-time, the product of the focus coefficients and weights can be used instead. Moreover, we hypothesized that eliminating out-of-focus weights in a trained network would produce a simplified and sparser network. For brevity, let us write ϕ_i for the focus coefficient i . By removing out-of-focus weights (by thresholding ϕ_i) we can prune the trained network. We demonstrated this on a focused network (Focused-s) trained on the MNIST dataset. Figure 4b shows the distribution of the number of non-zero connections per neuron in the first and second hidden layers achieved by the setting $\phi_i[\phi_i < 0.3] = 0$. After this pruning, the test accuracy was still unaffected (99.21). Most of the neurons were connected to almost half of the inputs (total=800) on average. Note that removing out-of-focus weights as described above differs from dropping smaller weights in a network.

Then, we examined the sparsity created by removing out-of-focus weights, in order to determine levels of tolerance to pruning. We calculated sparsity as the ratio of the number of zero weights to the number of total weights. Figure 4c plots the test set classification accuracy for increasing the sparseness value obtained by removing out-of-focus weights by an increasing threshold value t ($\phi_i[\phi_i < t] = 0$). The accuracy of the pruned network was still above the dense network even when more than 70% of the connections were dropped. Notably, it

was even possible to improve accuracy to a level slightly above the base training level.

4.4. *Non-spatial data*

The new model assumes a sort of ordered relationship (e.g., spatial, time) between inputs. Therefore, our primary tests were done on several commonly-used image datasets. However, it was important to confirm whether the model could function when dealing with non-spatial inputs. We aimed to determine this by testing it on Reuters-21578 news classification and Boston House price regression (both were available in Keras [29]) datasets. The Reuters data was pre-processed, inputs were converted to vectors of 1000 elements (following the steps in Reuters mlp example in [29]).

We then constructed a two hidden-layer network with 150 neurons in the hidden layers. We next trained the networks for 250 epochs with a stochastic mini-batch gradient descent of batch sizes 16 and 128 respectively for the Reuters and Boston sets. The first and second drop out layers used 0.2 and 0.25 probabilities, respectively. The Reuters training used the following learning rates: $\eta_g = 5e - 4$ and $\eta_{\mu,\sigma} = 1e - 3$, whereas the Boston training used $\eta_g = 5e - 3$ and $\eta_{\mu,\sigma} = 1e - 3$ for general and focus parameters, respectively. Every 30 epochs a decay of 0.9 was applied. The rightmost columns of Table 1 depict the results. In both datasets, the dense network accuracy was higher, followed by the Focus-s network. Figs. 3e and f show the training and validation set (test set for Boston) errors during training. However, two sample t-tests demonstrated that the mean differences between the dense network and focused-s network were insignificant, with values of ($t=1.35$, $p=0.21$; $t=-0.97$, $p=0.36$), respectively for the Reuters and Boston datasets.

4.5. Convolutional Networks

How would a convolutional network perform in our experimental setup with the same data? 2) How would the focusing neuron layers perform together with convolutional layers? To address these questions, we constructed a minimal convolutional network (CNN+Dns: Conv(32) - Conv(32)- Pool(2,2)- Drop(0.5)- Dense(256) - Drop(0.5) - Dense(10)). While the convolutional network had an additional layer to the previously compared networks, it had fewer parameters. The results are shown in the CNN+Dns row of Table 1. As expected, the CNN was superior to both the focusing and dense networks that were tested before. The gain was most prominent with the MNIST cluttered set (CLT), thanks to the translational invariance of CNN. However, in CIFAR-10 the gain was limited.

Then, we constructed a convolutional network where a focusing layer replaced the dense layer immediately after the convolutional layers (CNN+Fcs: Conv(32) - Conv(32)- Pool(2,2)- Drop(0.5)- Focus(256) - Drop(0.5) - Focus(10)). As the last row of Table 1 indicates, the results were almost equal in the MNIST set, in favor of the CNN+Dns in the Fashion set, and better for the focused CNN+Fcs in the MNIST-cluttered and CIFAR-10 sets.

T-tests: Again, we performed two-sample t-tests to see whether the difference in the mean test accuracies of the networks was significant. The second row of Table 2 compares CNN+Dns and CNN+Fcs networks. A significant difference was only observed with the MNIST-cluttered and CIFAR-10 datasets, in favor of the focused convolutional network.

4.6. Training and test time

The training time for the 2-hidden layer focusing network was up to two times longer than the dense network (See Section 4.2.1 for the configuration). The overhead was due to the extra gradient computations and parameter updates.

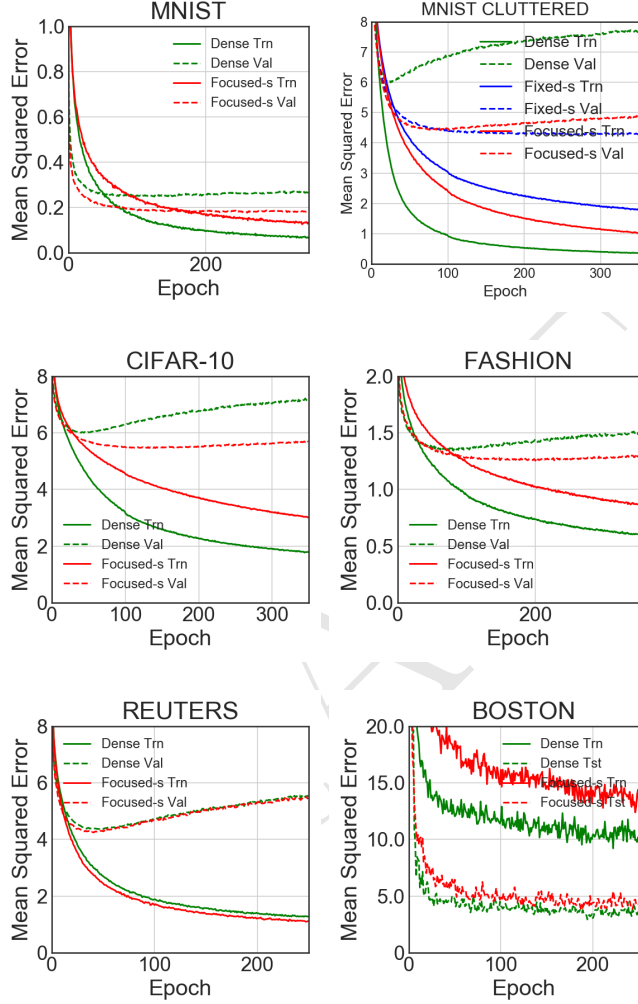


Figure 3: Training (Trn) and Validation (Val) mean squared error per training Epoch of Dense and Focused-s networks for a) MNIST, b) MNIST-cluttered, c) CIFAR-10, d) Fashion, e) Reuters, f) Boston (for Boston the train and test error plots are shown).

Table 1: Comparison of classification performance conducted on commonly-used datasets.

MNIST		CLT		CFR10		Fashion		Reuters		Boston	
Avg	Max	Avg	Max	Avg	Max	Avg	Max	Avg	Max	Avg	Min
Dense	98.96±.04	99.03	63.59±.21	63.98	58.99±.18	59.29	90.57±.12	90.69	79.63±.41	80.28	5.59±.36
Fixed-s	99.12±.03	99.15	73.48±.27	73.89	61.21±.3	61.53	89.66±.16	89.92	78.25±.52	79.03	10.94±.15
Focus-c	99.02±.06	99.10	67.94±.3	68.05	60.58±.4	61.04	90.56±.1	90.66	79.1±.55	79.92	6.56±.74
Focus-s	99.13±.06	99.21	72.24±.33	72.74	61.76±.3	62.26	90.8±.2	91.2	79.53±.44	80.05	5.79±.46
CNN+Dns	99.54±.05	99.61	93.19±.14	93.39	61.81±.48	62.56	93.21±.13	93.37	-	-	-
CNN+Fcs	99.52±.05	99.61	94.05±.29	94.54	62.64±.35	63.05	93.01±.14	93.23	-	-	-

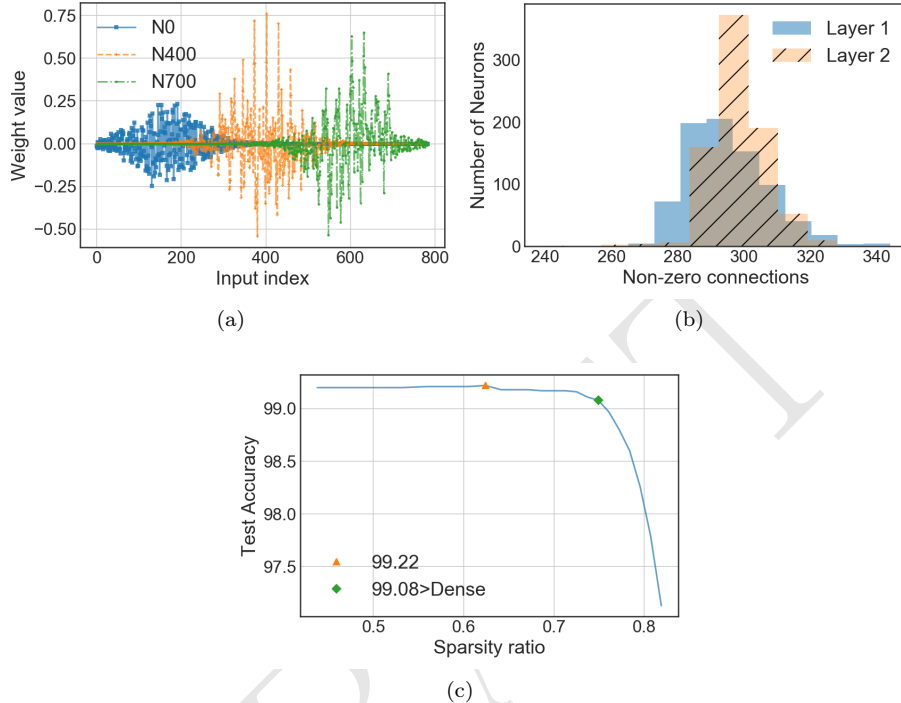


Figure 4: Focus-s network locality and sparsity after MNIST training. a) Focused weight values for three different neurons. b) The distribution of the number of non-zero connections in layer1/layer2 neurons by removing out-of-focus weights with $\phi_i[\phi_i < 0.3] = 0$, c) Test set accuracy for increasing sparsity obtained with increasing out-of-focus threshold t . The unpruned focused network performance was 99.21 at MNIST test set.

Table 2: Two-tailed two sample t-test comparison of the test results for Dense (Dense) vs. Focused network, and Convolutional Network with Dense layers (CNN+Dns) vs. the same with Focused Layers (CNN+Fcs). N=5, diff:mean difference, t: t-value, p: p-value (*significance).

	MNIST			CLT			CFR10			FASHION		
	diff	t	p (sig.)	diff	t	p (sig.)	diff	t	p (sig.)	diff	t	p (sig.)
Dense - Focused-s	-0.17	-7.08	0.0001*	-8.64	-44.09	7e-11*	-2.76	-15.6	2.8e-7*	-0.23	-2.01	0.078
CNN+Dns - CNN+Fcs	0.02	0.43	0.67	-0.85	-4.39	0.003*	-0.82	-2.79	0.023*	0.19	2.08	0.070

In MNIST, an epoch of 10000 instances, a batch size of 500, 28x28 inputs, took ≈ 0.63 s for the focusing network and ≈ 0.33 s for the dense network while running on an NVIDIA Tesla K40 GPU. The testing time difference (≈ 0.056 s vs. ≈ 0.053 s) was negligibly small as the only overhead was the calculation of the focus coefficients. However, after the training is finalized, the product of focus coefficients and weights can be stored as the final weight values to remove this small overhead.

5. Discussion

The experiments demonstrated that focusing neurons can change and learn their local receptive field regions and sizes. This capacity enabled the neurons to focus on informative features and steer away from the redundant-noisy inputs.

We compared a network of fully connected layers to a network of focusing neuron layers. In common image recognition datasets, the focused networks demonstrated significantly better than the dense networks, especially in more noisy and difficult domains such as MNIST-cluttered and CIFAR10.

The focusing neuron model is not designed for feature extraction. It is not expected to compete with convolutional kernels which use shared weights to their advantage for feature extraction. However, the experiments demonstrated that the focusing layers produced significantly better results when they replaced the dense layers in a convolutional network.

We have seen that focusing neurons can establish local connections. However, a focusing neuron is limited by its aperture of the whole input field. It contributes to the minimization of global errors by adapting to the local cues given by the local gradient. Though the focus parameters are only updated at the neuron level, we have witnessed collective partitioning of the whole input domain in several cases.

A focusing neuron is equipped with three different parameters -weights, σ , μ to control the magnitude of the incoming signal. Still, it is slightly more resistant to overfitting than a fully connected neuron because the receptive field is local. However, we observed overfitting tendencies at some enlarged weights. As in a fully connected neuron, additional regularization schemes can be used to compensate for the tendency to overfit.

From a biological perspective, it may be irrelevant to compare the different neuronal models because the brain has different types of nerve cells [39, 79]. Brain networks are formed of many local clusters with dense and short-path connections and few long-range connections linking those clusters [4]. Hence, the role of a focusing neuron can be different from the ones that are usually assigned to a fully connected neuron.

5.1. Limitations of the Study

Our implementation of the focusing neuron was 1-Dimensional. We speculate that a 2D implementation would perform better in 2D image recognition tasks. In addition, due to the limitations of our hardware, the architectures tested in the experiments were shallow compared to the state-of-the-art deep networks. We shall test the focusing neurons with deeper networks on larger data sets in different problems.

Finally, we tested the focusing layers against dense layers in common pattern recognition tasks. However, we believe that focusing neurons can be used to partition and distribute input spaces. To test this capacity, we must design experiments in which input is complex (multi-domain), such as, a part of the input carries speech signals while another part receives visual signals.

6. Conclusion

We have presented a new neuron model capable of learning its local receptive field region and size in the topological domain of its inputs. The new neuron model gains these abilities with a focus attachment. Though our choice of Gaussian focus control acts on a group/region of connected neurons, one can choose other differentiable functions.

In synthetic and some real image recognition data sets we demonstrated that focusing neurons can train their local receptive fields, which provides better generalization performance and sparser connection structures. As replacement for dense layers we tested the focusing layers in convolutional networks and found that significant improvements can be obtained in the classification of challenging data sets.

We plan to extend this work by exploring 2D-3D focusing neurons/layers, different focus control functions, forward focusing/distributing neurons, dynamic focusing and routing, applications in recurrent networks, and modeling of multi-problem networks.

Acknowledgments

This work was supported by Isik University BAP-16A202 grant; and NVIDIA Academic Hardware grant with a Tesla K40 GPU unit.

Thanks to Mr. İlker Çam for his contributions in the early development of the model and the code. Thanks to Dr. Murat S. Ayhan and Dr. Olcay T. Yıldız for discussions on the model. Thanks to Dr. Mehmet Önal and Dr. Deniz Karlı for their comments on the weight initialization.

Appendix A. Weight Initialization

An important aspect of the weight initialization is to sustain the variance of the signals that propagate through the layers [80, 74, 73, 81]. Hence, we can state our objective as having the variance of the output y equal to the variance of the input x_i , $\text{Var}(y) = \text{Var}(x)$. We follow the approach and notation of [81] to derive an appropriate weight initialization scheme for the focusing neuron model. For our discussion, we can safely omit the activation-transfer function, because the focusing model has no extra effect on it. We assume x_i and w_i are both independent and identically distributed (i.i.d) variables and $\phi(\tau(i, \theta))$ (shortly $\phi(i)$) is a deterministic function of i . The weights will be identically sampled from a zero mean distribution; hence the expected value is zero $\mathbb{E}[w_i] = 0$. However, a second initialization scheme is possible if we allow non-identical distributions. Let us start by writing the variance of the output y in terms of the weights, inputs, and $\phi(i)$.

$$y = \sum_{i=1}^m w_i \phi(i) x_i + b \quad (\text{A.1})$$

$$\text{Var}(y) = \mathbb{E}[y^2] - \mathbb{E}^2[y] \quad (\text{A.2})$$

$$\text{Var}(y) = \mathbb{E} \left[\left(\sum_{i=1}^m w_i \phi(i) x_i \right)^2 \right] - \mathbb{E}^2 \left[\sum_{i=1}^m w_i \phi(i) x_i \right] \quad (\text{A.3})$$

Since x_i and w_i are independent and $\mathbb{E}[w_i] = 0$, the second term on the right reduces to 0. We further examine the first term,

$$\text{Var}(y) = \mathbb{E} \left[\left(\sum_{i=1}^m w_i \phi(i) x_i \right)^2 \right] \quad (\text{A.4})$$

$$\begin{aligned} \text{Var}(y) &= \sum_{i=1}^m \phi^2(i) \mathbb{E}[w_i^2] \mathbb{E}[x_i^2] + \\ &2 \sum_{i=1}^m \sum_{k=j}^m \phi(i) \phi(k) \mathbb{E}[x_i x_k w_i w_k] \end{aligned} \quad (\text{A.5})$$

Again since x_i, w_i, x_k, w_k , are all independent and since $\mathbb{E}[w_i] = 0$, the double summation in (A.5) reduces to 0. Therefore,

$$\text{Var}(y) = \sum_{i=1}^m \phi^2(i) \mathbb{E}[w_i^2] \mathbb{E}[x_i^2] \quad (\text{A.6})$$

Now, we can simplify the notation by writing $s_{w_i}^2, s_{x_i}^2, s_y^2$ for the variances of the weight i , input i , and output y , respectively. In addition, μ_{x_i} denotes the mean for input i . Remember that weights are sampled from zero mean $\mu_{w_i} = 0$.

We can rewrite (A.6) as

$$s_y^2 = \sum_{i=1}^m \phi^2(i) (s_{w_i}^2) (s_{x_i}^2 + \mu_{x_i}^2) \quad (\text{A.7})$$

Now, we set constant variance for y (e.g., $s_y^2 = 1$) to solve the weight variance in two different ways. Remember that x_i are identical, so $\mu_{x_i} = \mu_x$ and $s_{x_i} = s_x$. First, we assume identical distribution and equal variance for the weights (i.e., $s_{w_i}^2 = s_{w_k}^2 = s_w^2$). Thus, the variance of each weight can be expressed as:

$$s_w^2 = \frac{1}{(s_x^2 + \mu_x^2) \sum_{i=1}^m \phi^2(i)} \quad (\text{A.8})$$

If we set $s_x^2 = 1$ and $\mu_x^2 = 0$, $s_{w_i}^2$ reduces to one over the squared norm of the ϕ coefficient vector. However, instead of equal variance weights, one can sample the weights non-identically from different distributions to create equal variance in the products $w_i * \phi(i)$. For example, if each term in the summation (A.7) receives $1/m$ variance, for a total variance of 1, we can initialize the independent weights with the following variance:

$$s_{w_i}^2 = \frac{1}{m(s_x^2 + \mu_x^2) \phi^2(i)} \quad (\text{A.9})$$

The different transfer functions require different scalers to provide the expected output variance [81, 73]. We used (A.8) and sampled the weights uniformly with $U[-\sqrt{6}/s_w, \sqrt{6}/s_w]$ for the rectified linear unit activation functions.

References

References

- [1] C. D. Gilbert, W. Li, V. Piech, Perceptual learning and adult cortical plasticity, *The Journal of Physiology* 30 (2009) 2743–2751.
- [2] M. M. Merzenich, T. M. V. Vleet, M. Nahum, Brain plasticity-based therapeutics, *Frontiers in Human Neuroscience* 8 8 (2014) 335.
- [3] J. D. Power, D. A. Fair, B. L. Schlaggar, S. E. Petersen, The development of human functional brain networks, *Neuron* 67 (2010) 735–748.
- [4] V. Menon, *Large-Scale Functional Brain Organization*, Elsevier, 2015, pp. 449–459.
- [5] S. Bartunov, A. Santoro, B. A. Richards, G. E. Hinton, T. Lillicrap, Assessing the scalability of biologically-motivated deep learning algorithms and architectures, *arXiv e-prints* 1807.04587v1.
- [6] C. Szegedy, S. Ioffe, V. Vanhoucke, A. Alemi, Inception-v4, inception-resnet and the impact of residual connections on learning, *arXiv1602.07261v2*.
- [7] G. Larsson, M. Maire, G. Shakhnarovich, Fractalnet: Ultra-deep neural networks without residuals, in: *ICLR* 2017, 2017.
- [8] G. Urban, Do deep convolutional nets really need to be deep and convolutional?, *ICLR*.
- [9] R. K. Srivastava, K. Greff, J. Schmidhuber, Highway networks, in: *ICML Deep Learning workshop*, 2015.
- [10] K. Xu, J. L. Ba, R. K. et al., Show, attend and tell: Neural image caption generation with visual attention, in: *Proc. of the 32nd ICML*, Vol. 37, 2015, pp. 2048–2057.
- [11] J. Ba, V. Mnih, K. Kavukcuoglu, Multiple object recognition with visual attention, *arXiv* 1412.7755. [arXiv:1412.7755v2](https://arxiv.org/abs/1412.7755).
- [12] O. Vinyals, A. Toshev, S. Bengio, D. Erhan, Show and tell: A neural image caption generator, in: *IEEE CVPR*, 2015.
- [13] D. Floreano, P. Dürr, C. Mattiussi, Neuroevolution: from architectures to learning, *Evolutionary Intelligence* 1 (1) (2008) 47–62.

- [14] A. Soltoggio, K. O. Stanley, S. Risi, Born to learn: the inspiration, progress, and future of evolved plastic artificial neural networks, *Neural Networks* 108 (2018) 48–67.
- [15] A. Romero, N. Ballas, S. E. Kahou, A. Chassang, C. Gatta, Y. Bengio, Fitnets: Hints for thin deep nets, in: ICLR, 2015.
- [16] B. Baker, O. Gupta, N. Naik, R. Raskar, Designing neural network architectures using reinforcement learning, in: ICLR, 2017.
- [17] H. Liu, K. Simonyan, Y. Yang, Darts: Differentiable architecture search, arXiv 1806.09055.
- [18] A. Coates, A. Y. Ng, Selecting receptive fields in deep networks, in: NIPS, 2011.
- [19] E. Fiesler, Comparative bibliography of ontogenetic neural networks, in: ICANN, Springer, 1994.
- [20] B. Hassibi, D. G. Stork, G. J. Wolff, Optimal brain surgeon and general network pruning, in: IEEE Int. Conf. on Neural Networks, Vol. 1, 1993, pp. 293–299.
- [21] S. Han, J. Pool, J. Tran, W. J. Dally, Learning both weights and connections for efficient neural networks, in: Proc. of the 28th Int. Conf. on Neural Information Processing Systems, 2015, pp. 1135–1143.
- [22] C. Cortes, X. Gonzalvo, V. Kuznetsov, M. Mohri, S. Yang, Adanet: Adaptive structural learning of artificial neural networks, in: Proc. of the 34th ICMLR, Vol. 70, 2017, pp. 874–883.
- [23] T. Serre, L. Wolf, S. Bileschi, M. Riesenhuber, T. Poggio, Robust object recognition with cortex-like mechanisms, *IEEE transactions on pattern analysis and machine intelligence* 29 (2007) 411–26. doi:10.1109/TPAMI.2007.56.
- [24] T. Masquelier, T. Serrea, S. Thorpe, T. Poggio, Learning simple and complex cells-like receptive fields from natural images: a plausibility proof, *Journal of Vision* 7 (2007) 81.
- [25] B. A. Olshausen, D. J. Field, Emergence of simple-cell receptive field properties by learning a sparse code for natural images, *Nature* 381 (1996) 607–609.
- [26] E. Stoeckli, Where does axon guidance lead us?, *F1000Research* 6 (78).
- [27] T. A. Suter, Z. J. DeLoughery, A. Jaworski, Meninges-derived cues control axon guidance, *Developmental Biology* 430 (2017) 1–10.

- [28] I. Çam, F. B. Tek, Odaklanan nöron (focusing neuron), in: 25th Signal Processing and Communications Applications Conference (SIU), 2017, pp. 1–4. doi:10.1109/SIU.2017.7960632.
- [29] F. e. a. Chollet, Keras, <https://github.com/fchollet/keras> (2015).
- [30] D. . T. W. Hubel, Receptive fields, binocular interaction and functional architecture in the cat's visual cortex., *J Physiol* 160 (1962) 106–54.
- [31] L. Chang, D. Y. Tsao, The code for facial identity in the primate brain, *Cell* 169 (2017) 1013–1028.
- [32] T. Poggio, T. Serre, Models of visual cortex, *Scholarpedia* 8 (4) (2013) 3516, revision #149958. doi:10.4249/scholarpedia.3516.
- [33] D. O. Hebb, *The Organization of Behaviour*, John Wiley & Sons, 1949.
- [34] P. Baldi, P. Sadowski, A theory of local learning, the learning channel, and the optimality of backpropagation, *Neural Networks* 83 (2016) 51–74.
- [35] F. Rosenblatt, The perceptron: A probabilistic model for information storage and organization in the brain, cornell aeronautical laboratory, *Psychological Review* 65 (6) (1958) 386–408.
- [36] Perceptrons, M.L. Minsky and S.A. Papert, MIT Press., Cambridge, MA, 1969.
- [37] S. M. K. Fukushima, T. Ito, Neocognitron: A neural network model for a mechanism of visual pattern recognition, *IEEE Trans. Systems, Man, and Cybernetics* 13 (1983) 826–834.
- [38] Y. LeCun, L. Bottou, Y. Bengio, P. Haffner, Gradient-based learning applied to document recognition, in: Proc. of the IEEE, Vol. 86, 1998, pp. 2278–2324.
- [39] S. Haykin, *Neural Networks: A Comprehensive Foundation*, 2nd Edition, Prentice Hall PTR, Upper Saddle River, NJ, USA, 1998.
- [40] M. T. Hagan, H. B. Demuth, M. H. Beale, *Neural Network Design*, Martin Hagan, 2014.
- [41] Y. LeCun, J. S. Denker, S. A. Solla, Optimal brain damage, in: D. S. Touretzky (Ed.), *Advances in Neural Information Processing Systems 2*, Morgan-Kaufmann, 1990, pp. 598–605.
- [42] D. Elizondo, R. Fiesler, A survey of partially connected neural networks., *Int J. Neural Systems* 8 (1997) 535–568.
- [43] A. G. Howard, M. Zhu, B. Chen, D. Kalenichenko, W. Wang, T. Weyand, M. Andreetto, H. Adam, Mobilenets: Efficient convolutional neural networks for mobile vision applications, arXiv abs/1704.04861.

- [44] S. Han, H. Mao, W. J. Dally, Deep compression: Compressing deep neural networks with pruning, trained quantization and huffman coding, arXiv 1510.00149.
- [45] F. Manessi, A. Rozza, S. Bianco, P. Napoletano, R. Schettini, Automated pruning for deep neural network compression, arXiv abs/1712.01721.
- [46] J. Wu, C. Leng, Y. Wang, Q. Hu, J. Cheng, Quantized convolutional neural networks for mobile devices, in: Proceedings of the IEEE Conference on Computer Vision and Pattern Recognition, 2016, pp. 4820–4828.
- [47] I. GoodFellow, Y. Bengio, A. Courville, Deep Learning, The MIT Press, 2016.
- [48] S. Y. Kung, J. N. Hwang, S. W. Sun, Efficient modeling for multilayer feed-forward neural nets, in: Int. Conf. on Acoustics, Speech, and Signal Proc., Vol. 4, 1988, pp. 2160–2163.
- [49] Y. LeCun, Generalization and network design strategies., Tech. Rep. CRG-TR-89-4, University of Toronto (1989).
- [50] Y. Taigman, M. Yang, M. Ranzato, L. Wolf, Deepface: Closing the gap to human-level performance in face verification, 2014 IEEE Conf. on Computer Vision and Pattern Recognition (2014) 1701–1708.
- [51] H. A. Rowley, S. Baluja, T. Kanade, Neural network-based face detection, IEEE Trans. Pattern Anal. Mach. Intell. 20 (1998) 23–38.
- [52] K. Gregor, Y. LeCun, Emergence of complex-like cells in a temporal product network with local receptive fields, arXiv abs/1006.0448.
- [53] S. Munder, D. M. Gavrila, An experimental study on pedestrian classification, IEEE Trans 28 (11) (2006) 1.
- [54] S. Sabour, N. Frosst, G. E. Hinton, Dynamic routing between capsules, arXiv abs/1710.09829.
- [55] L. Pang, Y. Lan, J. Xu, J. Guo, X. Cheng, Locally smoothed neural networks, CoRR abs/1711.08132.
- [56] I. Cam, F. B. Tek, Learning filter scale and orientation in cnns, arXiv preprint arXiv:1803.00388.
- [57] M. J. L. Orr, Introduction to radial basis function networks (1996).
- [58] T. Kohonen, Learning vector quantization, in: M. Arbib (Ed.), The Handbook of Brain Theory and Neural Networks, MIT Press, 1995.
- [59] T. Kohonen, The self-organizing map, Proceedings of the IEEE 78 (9) (1990) 1464–1480.

[60] U. Esposito, Investigating connectivity in brain-like networks, Ph.D. thesis, The University of Sheffield, UK (2016).

[61] U. Bodenhausen, A. Waibel, The tempo 2 algorithm: Adjusting time-delays by supervised learning, in: Proceedings of the 3rd International Conference on NIPS90, 1990, pp. 155–161.

[62] W. Gerstner, W. M. Kistler, Mathematical formulations of Hebbian learning, *Biol. Cybern.* 87 (404–415).

[63] J. Triesch, Synergies between intrinsic and synaptic plasticity mechanisms., *Neural Comput.* 19 (2007) 885–909.

[64] E. Oja, Simplified neuron model as a principal component analyzer, *Journal of Mathematical Biology* 15 (3) (1982) 267–273.

[65] T. Miconi, J. Clune, K. O. Stanley, Differentiable plasticity: training plastic networks with gradient descent, in: International Conference on Machine Learning, 2018.

[66] G. B. Huang, Z. Bai., L. Kasun, C. Vong, Local receptive fields based extreme learning machine., *IEEE Computational Intelligence Magazine* 10 (2015) 18–29.

[67] L. Itti, C. Koch, E. Niebur, A model of saliency-based visual attention for rapid scene analysis, *IEEE Trans. on PAMI* 20 (1998) 1254–1259.

[68] B. Olshausen, C. Anderson, D. Van Essen, A neurobiological model of visual attention and invariant pattern recognition based on dynamic routing of information, *Journal of Neuroscience* 13 (11) (1993) 4700–4719.

[69] B. Cheung, E. Weiss, B. A. Olshausen, Emergence of foveal image sampling from learning to attend in visual scenes, *CoRR* abs/1611.09430.
URL <http://arxiv.org/abs/1611.09430>

[70] Theano Dev. Team, Theano: A Python framework for fast computation of mathematical expressions, *arXiv e-prints* abs/1605.02688.

[71] M. Abadi, P. Barham, Tensorflow: A system for large-scale machine learning, in: 12th USENIX Symposium on Operating Systems Design and Implementation (OSDI 16), 2016, pp. 265–283.

[72] T. Lindeberg, Generalized Gaussian scale-space axiomatics comprising linear scale-space, affine scale-space and spatio-temporal scale-space, *Journal of Mathematical Imaging and Vision* 40 (1) (2011) 36–81.

[73] K. He, X. Zhang, S. Ren, J. Sun, Delving deep into rectifiers: Surpassing human-level performance on imagenet classification, in: Proc. of the 2015 IEEE ICCV, 2015, pp. 1026–1034.

- [74] X. Glorot, Y. Bengio, Understanding the difficulty of training deep feed-forward neural networks, in: Proceedings of Machine Learning Research, Vol. 9, 2010, pp. 249–256.
- [75] Online (2018). [link].
URL <https://github.com/btekgit/FocusingNeuron.git>
- [76] M. Jaderberg, K. Simonyan, A. Zisserman, K. Kavukcuoglu, Spatial transformer networks, CoRR,arXiv abs/1506.02025.
- [77] A. Krizhevsky, Learning multiple layers of features from tiny images, Tech. rep., Canadian Institute For Advanced Research (2009).
- [78] H. Xiao, K. Rasul, R. Vollgraf, Fashion-mnist: a novel image dataset for benchmarking machine learning algorithms, arXiv cs.LG/1708.07747.
- [79] E. R. Kandel, In search of memory: The emergence of a New Science of Mind, W. W. Norton & Company, 2006.
- [80] Y. LeCun, L. Bottou, G. B. Orr, K.-R. Müller, Efficient BackProp, Springer, Heidelberg, 2012, pp. 9–48.
- [81] S. K. Kumar, On weight initialization in deep neural networks, arXiv abs/1704.08863.